NASA-CR-204367

VAPOR FLOW PATTERNS DURING A START-UP
TRANSIENT IN HEAT PIPES

F. Issacci, N. M. Ghoniem, and I. Catton
Department of Mechanical, Aerospace and Nuclear Engineering
University of California, Los Angeles
Los Angeles, California

ABSTRACT

The vapor flow patterns in heat pipes are examined during the start-up transient phase. The vapor core is modelled as a channel flow using a two dimensional compressible flow model. A nonlinear filtering technique is used as a post process to eliminate the non-physical oscillations of the flow variables. For high-input heat flux, multiple shock reflections are observed in the evaporation region. The reflections cause a reverse flow in the evaporation and circulations in the adiabatic region. Furthermore, each shock reflection causes a significant increase in the local pressure and a large pressure drop along the heat pipe.

NOMENCLATURE

b channel width
C_p specific heat
h_{fg} latent heat
k thermal conductivity
L heat pipe total length
L_a adiabatic section length
L_c condenser length
L_e evaporator length
$\dot{m}''$ mass flux
Nx number of grid points in x-direction
Ny number of grid points in y-direction
p pressure
$\dot{q}''$ input heat flux
R gas constant
Re Reynolds number
T Temperature
t time

u axial velocity
v vertical velocity
x axial coordinate
y vertical coordinate

δ liquid layer thickness
μ viscosity
ρ density
ϕ general dependent variable
ϕ^r referenced value of ϕ

Subscripts

c condenser
eff effective
o initial value
sat saturation

INTRODUCTION

The transient behavior of vapor flow during the start-up phase of heat pipe operation has been analyzed in order to examine the flow patterns for high-input heat fluxes. Start-up is a transient process through which the heat pipe starts its operation from a static condition and arrives at steady-state operation. During a start-up transient, the working fluid of a heat pipe may initially be very cold or frozen in the wick. Here, the liquid is assumed to be very cold and the vapor, which is thermodynamically in equilibrium with the liquid, is at very low pressure. The vapor core response to a sudden high-input heat flux is the primary focus of this work.

41

The past two-dimensional (2D) studies are limited to incompressible flows (Tien and Rohani, 1974; Faghri, 1986; and Peterson and Tien, 1987) and compressible flow studies are limited to 1D (e.g., Chen and Faghri, 1989). At UCLA, the study of dynamic behavior of heat pipes began by analyzing the liquid and vapor phases separately (Roche, 1988; Issacci et al., 1988). The objective was to develop very detailed computer codes for each phase and then to combine them in a comprehensive code. Roche (1988) developed a numerical code for the liquid phase at the start-up transient mode by assuming the vapor phase at a constant temperature and pressure. He used a kinetic theory approach to model the phase change at the liquid-vapor interface. The vapor dynamics of heat pipes was studied by Issacci et al. (1989) using a 2D transient model with the SIMPLER method (Patankar, 1980). The primary advantage of SIMPLER is the staggered grid which makes the numerical scheme very stable and, consequently, the computational time very low. Although this method yielded interesting results, the resulting computational code was limited to low compressibility flows. However, in the start-up mode of a heat pipe, there are regions of high as well as low compressibility.

A filtering technique, based on the concept introduced by Engquist et al. (1989), was used in a study of 1D compressible vapor dynamics by Issacci et al. (1990a). It was shown that the centered-difference scheme (CDS) used with nonlinear filtering yields a second order, stable solution in cell Reynolds problems and is able to capture a shock without oscillations. The same method was also used in a 2D analysis of vapor dynamics in heat pipes by Issacci et al. (1990b). The shock reflection in the evaporation region was observed to affect the flow pattern and the pressure drop along the pipe. This study is continued here for high-input heat fluxes. The corresponding Mach number is about one and the flow patterns show a strong flow circulation in the evaporation and adiabatic regions and, consequently, a large pressure drop along the heat pipe.

GOVERNING EQUATIONS

Vapor flow in the heat pipe core is modeled as channel flow, as is shown in Fig. 1. The bottom boundary of the channel is a thin porous medium which contains the liquid. The input heat flux to the evaporator and the temperature of the outer surface of the condenser are specified. The planar side walls are assumed adiabatic.

The equations governing the vapor flow are the continuity, momentum, and energy equations, which are time dependent, viscous, and compressible. An equation of state (EOS) is used to relate pressure,
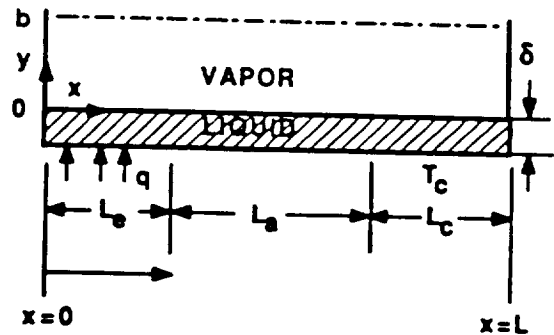

Fig. 1. Vapor flow model in a heat pipe

density, and temperature within the vapor core. These equations in Cartesian coordinates (x,y) are

Continuity

$$\frac{\partial \rho}{\partial t} + \frac{\partial (\rho u)}{\partial x} + \frac{\partial (\rho v)}{\partial y} = 0 \tag{1}$$

x-Momentum

$$\frac{\partial (\rho u)}{\partial t} + \frac{\partial (\rho u u)}{\partial x} + \frac{\partial (\rho u v)}{\partial y} = -\frac{\partial p}{\partial x} + \frac{\partial}{\partial x}\left(\mu \frac{\partial u}{\partial x}\right) + \frac{\partial}{\partial y}\left(\mu \frac{\partial u}{\partial y}\right)$$
$$+\left[\frac{\partial}{\partial x}\left(\mu \frac{\partial u}{\partial x}\right) + \frac{\partial}{\partial y}\left(\mu \frac{\partial v}{\partial x}\right) - \frac{2}{3}\frac{\partial}{\partial x}\left(\mu \frac{\partial u}{\partial x} + \mu \frac{\partial v}{\partial y}\right)\right] \tag{2}$$

y-Momentum

$$\frac{\partial (\rho v)}{\partial t} + \frac{\partial (\rho u v)}{\partial x} + \frac{\partial (\rho v v)}{\partial y} = -\frac{\partial p}{\partial y} + \frac{\partial}{\partial x}\left(\mu \frac{\partial v}{\partial x}\right) + \frac{\partial}{\partial y}\left(\mu \frac{\partial v}{\partial y}\right)$$
$$+\left[\frac{\partial}{\partial x}\left(\mu \frac{\partial u}{\partial y}\right) + \frac{\partial}{\partial y}\left(\mu \frac{\partial v}{\partial y}\right) - \frac{2}{3}\frac{\partial}{\partial y}\left(\mu \frac{\partial u}{\partial x} + \mu \frac{\partial v}{\partial y}\right)\right] \tag{3}$$

Energy

$$C_p\left[\frac{\partial (\rho T)}{\partial t} + \frac{\partial (\rho u T)}{\partial x} + \frac{\partial (\rho v T)}{\partial y}\right] = \frac{\partial p}{\partial t} + u\frac{\partial p}{\partial x} + v\frac{\partial p}{\partial y} + \frac{\partial}{\partial x}\left(k\frac{\partial T}{\partial x}\right)$$
$$+ \frac{\partial}{\partial y}\left(k\frac{\partial T}{\partial y}\right) + \mu\left[2\left(\frac{\partial u}{\partial x}\right)^2 + 2\left(\frac{\partial v}{\partial y}\right)^2 + \left(\frac{\partial u}{\partial y} + \frac{\partial v}{\partial x}\right)^2\right] \tag{4}$$

EOS

$$p = \rho R T \tag{5}$$

Initial and Boundary Conditions

The working liquid is assumed initially to be at a very low temperature (close to the freezing point). Further, there is no input heat and the stagnant vapor is in thermodynamic equilibrium with the

42

liquid. The boundaries of the vapor core are shown in Fig. 1. A no-slip condition for the velocity and an adiabatic condition for the temperature are assumed on the side walls, i.e., at $x = 0$ and $x = L$.

$$u = 0 \quad , \quad v = 0 \quad , \quad \partial T / \partial x = 0 \qquad (6)$$

On the center line the symmetry condition implies, at $y = b$,

$$\partial u / \partial y = 0 \quad , \qquad v = 0 \quad , \qquad \partial T / \partial y = 0 \qquad (7)$$

The boundary conditions at the liquid-vapor interface are the challenging ones. The liquid flow is assumed to be in a porous medium of thickness, δ, which is much smaller than the vapor core thickness, b. The axial velocity is assumed zero on this boundary, i.e., at $y = 0$,

$$u = 0 \qquad (8)$$

To assign boundary conditions for the temperature and vertical velocity, the liquid-vapor interface is divided into three regions. In the evaporation zone the input flux, $\dot{q}''$, is a given parameter and the input flow is approximated at $y = 0$ and $0 < x \leq L_e$ by

$$\rho v = \dot{m}'' = \dot{q}'' / h_{fg}(T) \quad , \quad T = T_{sat}(p) \qquad (9)$$

where h_{fg} is the heat of vaporization and $\dot{m}''$ is the input mass flux. Conduction in the liquid layer is neglected. It should be noted that this boundary condition ignores the thermal characteristics of the heat pipe wall and the working fluid-wick layer. The temperature is assumed to be the saturation temperature of the liquid corresponding to the interface pressure, $T_{sat}(p)$. In the adiabatic zone, the boundary conditions at $y = 0$ and $L_e < x \leq (L_e + L_a)$ are

$$v = 0 \quad , \quad \partial T / \partial y = 0 \qquad (10)$$

In the condensation zone the temperature of the outer surface, T_c, is given. By equating the heat of evaporation to the heat conduction in the liquid layer, the outflow from this region is approximated at $y = 0$ and $(L_e + L_c) < x \leq L$, by

$$\rho v = \dot{m}'' = -\frac{k_{eff}}{\delta}\left(\frac{T-T_c}{h_{fg}(T)}\right) \quad , \quad T = T_{sat}(p) \qquad (11)$$

where k_{eff} is the effective conductivity of the liquid layer and the temperature is assumed to be the saturation temperature corresponding to the

pressure at the interface. This neglects transient conduction in the fluid layer which may be an important contribution to the process.

SOLUTION METHOD

The five governing equations, (1)-(5), with the initial and boundary conditions given by equations (6)-(11), have been solved numerically for the five variables: ρ, ρu, ρv, T, and p. A finite-difference method has been used with backward Euler discretization in time and centered differences in space. Dealing with a wide range of input heat fluxes, the method deals effectively with the cell Reynolds-number problem as well as shock-capturing complexity. Discretization of the advective terms in this problem plays a significant role. The centered-difference scheme (CDS) is ill-behaved for grid Reynolds numbers larger than two because the coefficients of the difference equations are not necessarily positive. As a consequence, solutions to the difference equations may not be unique, resulting in nonphysical spatial oscillations. In a study of the 1D forms of the governing equations, (1)-(5), by Issacci et al. (1990a), standard methods such as upwinding and power law and a more recent scheme, CONDIF, were examined. It was shown that these schemes are well-behaved but that they cause oscillations and overshoot at high compressibility and, except for CONDIF, they cause high numerical diffusion at low compressibility as well. The CONDIF scheme was used by Issacci et al. (1990c) in a study of the start-up transient process in heat pipes. It was shown that for input heat fluxes > 1 kW/m² in an Na-filled heat pipe, a shock is created in the evaporation region. Therefore, the CONDIF scheme was found to be unsuitable for shock capturing.

In the present work the same technique used in the study by Issacci et al. (1990a,b) has been used to solve the 2D form of the governing equations for a compressible vapor flow. The governing equations are nonlinear and coupled. An iterative method is used to solve each equation separately, i.e., equations (1)-(5) for ρ, ρu, ρv, T, and p, respectively. The SOR method is used to solve the differenced equations. Iteration on the equations were stopped after convergence of all the variables. This iteration method required the least storage and fewest calculations.

RESULTS

For the results shown in this section, the working fluid is liquid sodium at, initially, $P_o = 10^{-2}$ atm and $T_o = 800$ K. The geometry dimensions are $b = 5$ cm, $L_e = L_a = L_c = b$. The calculational grid for each computation was chosen by inspection of the

calculated L^2-norm error. The L^2-norm is defined as

$$L^2 - norm = \left[\frac{1}{NxNy}\sum_{i,j}\left(\frac{\phi_{i,j}-\phi'_{i,j}}{\phi'_{i,j}}\right)^2\right]^{1/2} \qquad (12)$$

where Nx and Ny are numbers of grid points in x- and y-directions, respectively. Here, ϕ is one of the dependent variables $(\rho, \rho u, \rho v, T,$ or $P)$ and ϕ' is the calculated ϕ on the finest mesh of calculations.

Figure 2 shows the flow patterns in the vapor core for a high-input heat flux, $\dot{q}''_e = 10^6$ W/m². The Reynolds number based on the vapor thickness is $Re = 100$ and the computations were done for an optimized grid of 41 x 121. The transient development of the vertical mass flux, ρv, at different times is shown in Fig. 2. At $t = 0$, the vapor is stagnant. Applying the input heat flux, evaporation takes place in the evaporator $0 < x/b \leq 1$. Since the input heat flux is high, a shock wave is created (Fig. 2a). The vapor flow develops above the evaporator and in the adiabatic region and the shock travels above the evaporator until it hits the upper boundary (Fig. 2b) where the vertical mass flux is blocked, $\rho v = 0$. At this point, the vapor is compressed and the vapor pressure increases which causes a positive vertical pressure gradient and the shock reflects back (Fig. 2c). The figure also shows reverse flow in the top left corner which is caused by shock reflection. When the reflected shock reaches the lower boundary (Fig. 2d) and the vapor is compressed within the evaporation region, the vertical pressure gradient is reduced and the inflow mass flux tries again to fill the evaporation region (Fig. 2e). As the vapor fills the evaporation region, another shock reflection occurs. Each reflection of the shock wave causes a significant increase in the local pressure and, consequently, a large pressure drop along the heat pipe.

The same multiple shock reflection and refill of vapor in the evaporator region was also observed with lower input heat flux, $\dot{q}''_e = 10^5$ W/m² (Issacci et. al. 1990b). However, at high-input heat flux ($\dot{q}''_e = 10^6$ W/m²), the flow pattern in the adiabatic region, $1 < x/b \leq 2$, is significantly different from that for lower heat fluxes. Figure 2d shows that when the shock reflection reaches the lower boundary of the evaporator, circulation is initiated in the adiabatic region. This circulation ceases when the vapor flow refills the evaporator region (Fig. 2e). However, the second reflection will cause a stronger circulation in the adiabatic region, as shown in Fig. 2f. Figures 2g through 2ℓ demonstrate the subsequent sets of reflection and refill of the vapor flow with circulation strength increasing with time. When the process reaches steady-state conditions, circulation occupies a significant portion of the

region. Circulation in the adiabatic region was also found and reported by Issacci et al. (1989) in an analysis of the operational transient mode of heat pipes.

In order to show the overall picture of flow pattern development, Fig. 3 was prepared to depict the vapor flow fields at different times. Figure 3a shows the flow field at an early stage of the transient process after the first shock reflection. Here the flow reversal is shown to be in the left top corner of the evaporation region. The shock reflection initiates flow circulation at the entrance to the adiabatic region shown in Fig. 3b. Vortex formation in the adiabatic region develops with time to a stronger flow circulation (Fig. 3c) and another vortex can be seen in the left corner of the evaporation region. In the flow field at steady state (Fig. 3d), it is seen that flow circulation in the adiabatic region develops to two vortices.

CONCLUSIONS

A nonlinear filtering technique has been used to analyze the start-up vapor dynamics in heat pipes. Large variations in vapor compressibility during the transient phase render it inappropriate to use the SIMPLER scheme or to use standard schemes for the discretization of advective terms.

For a high heat flux, the start-up transient phase involves multiple shock reflections from the line of symmetry in the evaporator region. Each shock reflection causes a significant increase in the local pressure and a large pressure drop along the heat pipe. Furthermore, shock reflections cause flow reversal in the evaporation region and flow circulations in the adiabatic region. The vapor vortex formation in the evaporator is only transient and is observed to disappear as the dynamics approach steady state. However the circulation in the adiabatic region grows with time, and in the steady-state condition the circulation occupies a significant portion of the region.

The pressure increase due to shock reflection may cause the overall pressure of the evaporator to be greater than the saturated vapor pressure. When this occurs, condensation takes place by mist nucleation in the vapor. Therefore, the condensation rate is expected to decrease.

The time for the vapor core to reach a steady-state condition depends on the input heat flux, the heat pipe geometry, the working fluid, and the condenser conditions. However, the vapor transient time is on the order of seconds. Depending on the time constant for the overall system, the vapor transient time may be very short. Therefore, the vapor core may be assumed quasi-steady in transient analysis of a heat pipe operation.
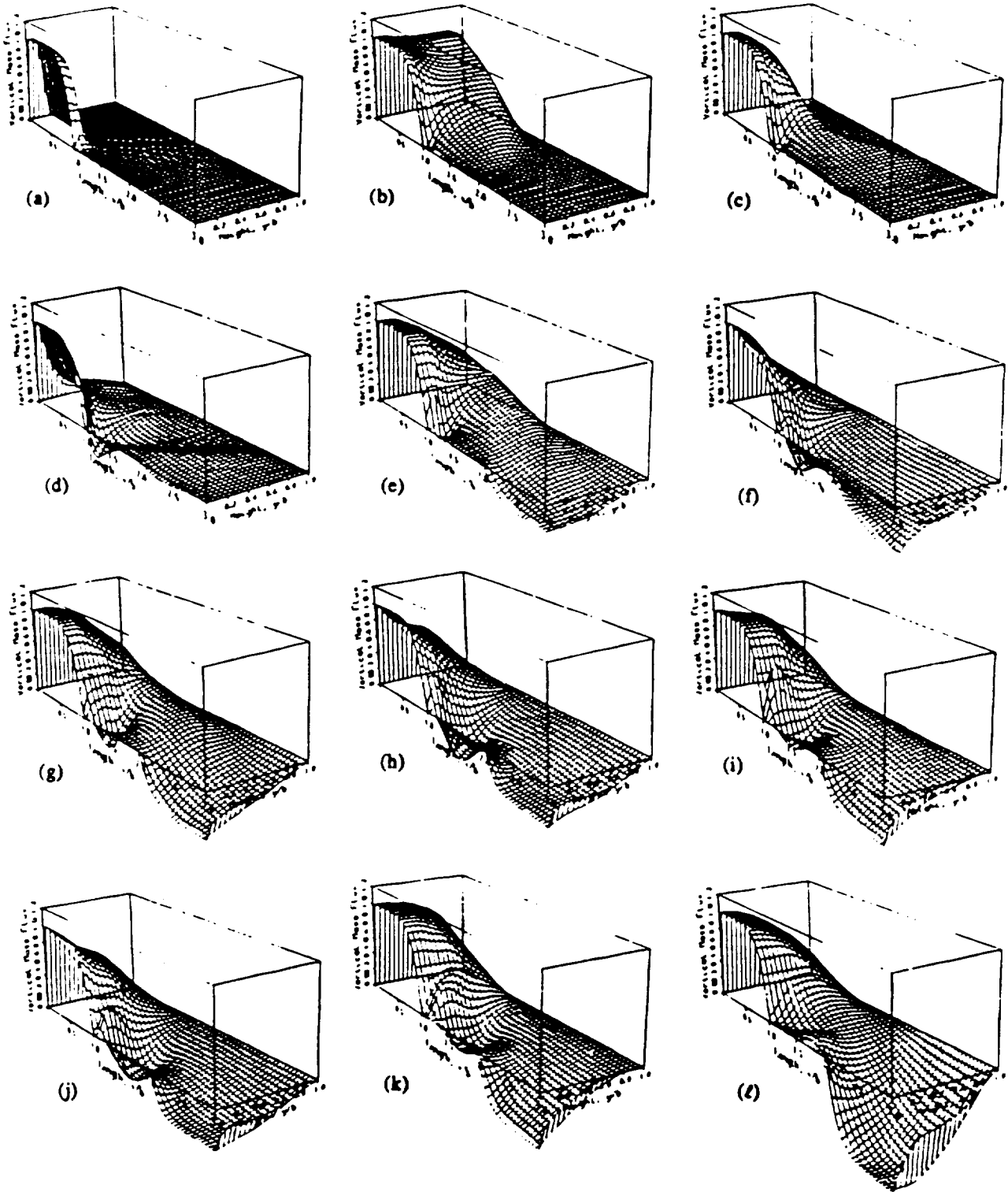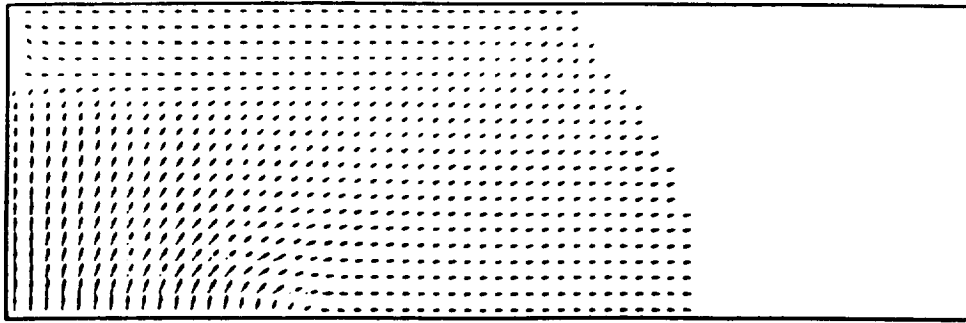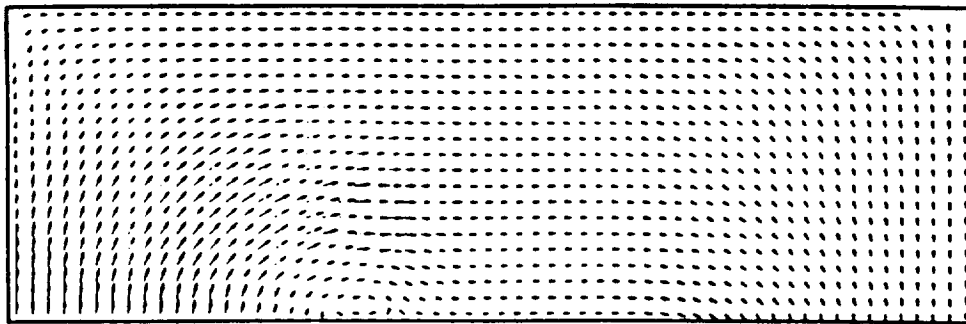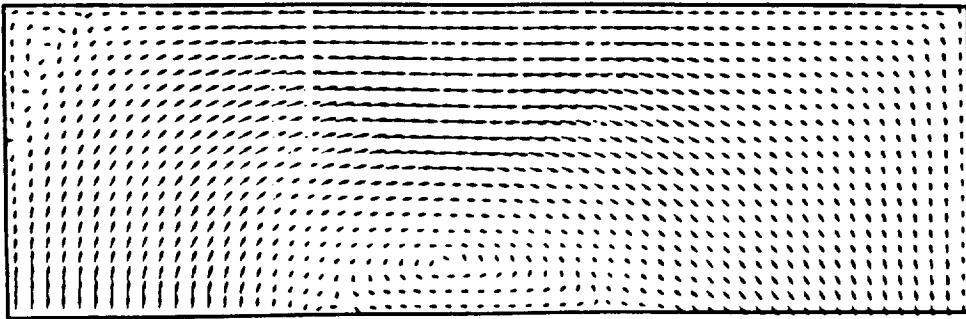
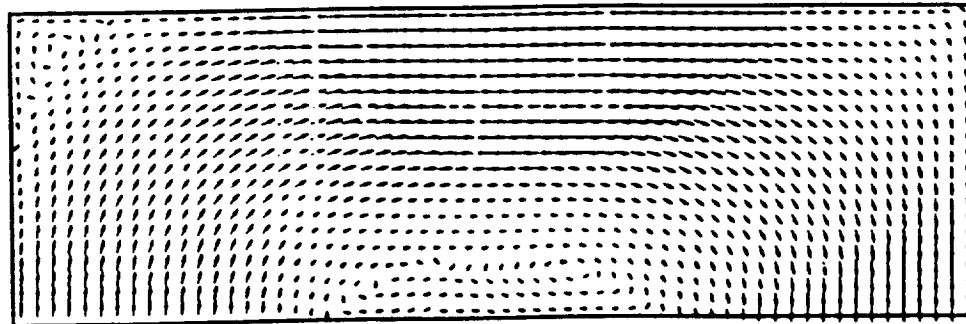Fig. 2. Transient development of the vertical mass flux: high-input heat flux

(a)

(b)

(c)

(d)

Fig. 3. Vapor flow fields at different times (arrows indicate direction: tail indicates magnitude)

ACKNOWLEDGMENT

REFERENCES

Engquist, B., Lötstedt, P., and Sjögreen, B., 1989, "Nonlinear Filters for Efficient Shock Computation," *J. Math. Comp.*, Vol. 52, No. 186, pp. 509-537.

Faghri, A., 1986, "Vapor Flow Analysis in a Double-Walled Concentric Heat Pipe," *Numerical Heat Transfer*, Vol. 10, pp. 583-596.

Issacci, F., Roche, G. L., Klein, D. B., and Catton, I., 1988, "Heat Pipe Vapor Dynamics," University of California Los Angeles, *Report No. UCLA-ENG-88-28.*

Issacci, F., Catton, I., Heiss, A., and Ghoniem, N. M., 1989, "Analysis of Heat Pipe Vapor Flow Dynamics," *Chem. Eng. Comm.*, Vol. 85, pp. 85-94.

Issacci, F., McDonough, J. M., Catton, I., and Ghoniem, N. M., 1990a, "Nonlinear Filtering for Shock Capturing and Cell-Reynolds Number Problems in Compressible Vapor Dynamics," *J. Comp. Phys.*, submitted.

Issacci, F., Catton, I., and Ghoniem, N. M., 1990b, "Start-up Transient Modeling of Vapor Flow in Heat Pipes," to be presented at *9th International Heat Transfer Conf.*, August 18-24, Jerusalem, Israel.

Issacci, F., Catton, I., and Ghoniem, N. M., 1990c, "Vapor Dynamics of Heat Pipe Start-up," *Proc., 7th Symp. on Space Nuclear Power Systems*, Vol. 2, pp. 1002-1007, Institute for Space Nuclear Power Studies, University of New Mexico.

Patankar, S. V., 1980, *Numerical Heat Transfer and Fluid Mechanics*, Mc-Graw Hill, New York.

Peterson, P. F., and Tien, C. L., 1987, "Gas-Concentration Measurements and Analysis for Gas-Loaded Thermosyphons,"*Proc., International Symp. on Natural Circulation*, ASME HTD, Boston, MA.

Roche, G. L., 1988, "Analytical Studies of the Liquid Phase Transient Behavior of a High Temperature Heat Pipe," M.S. Thesis, University of California Los Angeles.

Runchal, A. K., 1987, "CONDIF: A Modified Central-Difference Scheme for Convective Flows," *Int. J. Numer. Methods Eng.*, Vol. 24, No. 8, pp. 1593-1608.

Tien, C. L., and Rohani, A. R., 1974, "Analysis of the Effects of Vapor Pressure Drop on Heat Pipe Performance," *Int. J. Heat Mass Transfer*, Vol. 17, pp. 61-67.